Title

Material/element-dependent fluorescence-yield modes on soft X-ray absorption spectroscopy of cathode materials for Li-ion batteries

Journal

AIP Advances, 6(3)

ISSN

2158-3226

Authors

Asakura, Daisuke
Hosono, Eiji
Nanba, Yusuke
et al.

Publication Date

2016-03-01

DOI

10.1063/1.4943673

Peer reviewed

Material/element-dependent fluorescence-yield modes on soft X-ray absorption spectroscopy of cathode materials for Li-ion batteries

Daisuke Asakura, Eiji Hosono, Yusuke Nanba, Haoshen Zhou, Jun Okabayashi, Chunmei Ban, Per-Anders Glans, Jinghua Guo, Takashi Mizokawa, Gang Chen, Andrew J. Achkar, David G. Hawthron, Thomas Z. Regier, and Hiroki Wadati

Citation: AIP Advances **6**, 035105 (2016); doi: 10.1063/1.4943673

View online: http://dx.doi.org/10.1063/1.4943673

View Table of Contents: http://aip.scitation.org/toc/adv/6/3

Published by the American Institute of Physics

Material/element-dependent fluorescence-yield modes on soft X-ray absorption spectroscopy of cathode materials for Li-ion batteries

Daisuke Asakura,[1,a] Eiji Hosono,[1] Yusuke Nanba,[1,b] Haoshen Zhou,[1] Jun Okabayashi,[2] Chunmei Ban,[3] Per-Anders Glans,[4] Jinghua Guo,[4,5] Takashi Mizokawa,[6,c] Gang Chen,[7] Andrew J. Achkar,[8] David G. Hawthron,[8] Thomas Z. Regier,[9] and Hiroki Wadati[10]

[1]*Energy Technology Research Institute, National Institute of Advanced Industrial Science and Technology, Tsukuba, Ibaraki 305-8568, Japan*
[2]*Research Center for Spectrochemistry, The University of Tokyo, Bunkyo-ku, Tokyo, 113-0033, Japan*
[3]*The Chemical and Materials Science Center, National Renewable Energy Laboratory, Golden, Colorado, 80401, USA*
[4]*Advanced Light Source, Lawrence Berkeley National Laboratory, Berkeley, California, 94720, USA*
[5]*Department of Chemistry and Biochemistry, University of California, Santa Cruz, California, 95064, USA.*
[6]*Department of Complexity Science and Engineering, The University of Tokyo, Kashiwa, Chiba, 277-8561, Japan*
[7]*College of Physics/State Key Laboratory of Superhard Materials, Jilin University, Changchun, 130012, People's Republic of China*
[8]*Department of Physics and Astronomy, University of Waterloo, Waterloo, Ontario, N2L 3G1, Canada*
[9]*Canadian Light Source, University of Saskatchewan, Saskatoon, Saskatchewan, S7N 0X4, Canada*
[10]*Institute for Solid State Physics, The University of Tokyo, Kashiwa, Chiba, 277-8581, Japan*

(Received 1 December 2015; accepted 25 February 2016; published online 7 March 2016)

We evaluate the utilities of fluorescence-yield (FY) modes in soft X-ray absorption spectroscopy (XAS) of several cathode materials for Li-ion batteries. In the case of total-FY (TFY) XAS for $LiNi_{0.5}Mn_{1.5}O_4$, the line shape of the Mn L_3-edge XAS was largely distorted by the self-absorption and saturation effects, while the distortions were less pronounced at the Ni L_3 edge. The distortions were suppressed for the inverse-partial-FY (IPFY) spectra. We found that, in the cathode materials, the IPFY XAS is highly effective for the Cr, Mn, and Fe L edges and the TFY and PFY modes are useful enough for the Ni L edge which is far from the O K edge.
[http://dx.doi.org/10.1063/1.4943673]

Electronic-structure analyses for the electrode materials of Li-ion batteries (LIBs) are essential to understand the charge-discharge properties, which is capable of leading to improvements of the battery performance. The 3*d* transition metals (TMs) are the major elements in the cathode materials for LIBs, such as TM oxides and phosphates. The TMs in the LIBs cathode materials experience the oxidation and reduction during charging/discharging process (i.e. Li-ion extraction/insertion). The redox chemistry determines the electrochemical properties of the electrode materials. Thus, element-selective electronic-structure analyses are indispensable for the application of LIBs.

[a]Author to whom correspondence should be addressed. Electronic mail: daisuke-asakura@aist.go.jp
[b]Present affiliation: Inamori Frontier Research Center, Kyushu University, Fukuoka, 819-0395, Japan
[c]Present affiliation: Department of Applied Physics, Waseda University, Tokyo, 169-8555, Japan

In LIB research, TM K-edge X-ray absorption spectroscopy in hard X-ray region is widely used to investigate the electronic structures of cathode materials.[1,2] The redox reactions of TMs can be clarified by the edge/peak shift in the TM K-edge absorption spectra. However, the TM K-edge X-ray absorption spectroscopy is less sensitive to the 3d electronic states of TMs than the TM $L_{2,3}$-edge (i.e. the 2p-3d transition) X-ray absorption spectroscopy, because the 1s-4p dipole transition is dominant at the TM K edges.

To obtain the detailed information of the 3d orbitals, i.e. electronic-structure parameters such as charge-transfer energy, soft X-ray absorption spectroscopy (XAS) covering the TM $L_{2,3}$ edges (i.e. the 2p-3d transition) has been widely used for various fields including solid state physics.[3,4] Total-electron yield (TEY) is the most conventional detection mode for the XAS experiments in the soft X-ray region, while the probing depth is approximately 5 nm at most. The surface sensitivity of the TEY mode is frequently inappropriate for investigating the redox reaction in the cathode materials. In contrast, total-fluorescence-yield (total FY: TFY) XAS can probe the bulk electronic structures as deep as ~100 nm from the sample surface. However, the TM L_3-edge TFY XAS spectra tend to be distorted by self-absorption and saturation effects.[5] These effects are dependent on the density, particle size (for powder) and thickness (for thin film) of the sample and the measurement geometry such as normal/grazing incidence. In addition, the distortion in the line shapes of TM L_3-edge TFY XAS is enhanced in case where the target sample does not contain heavy elements such as rare earth.[6] Thus, powdered Li-TM oxides and related compounds used for cathode materials of LIB are frequently affected by these effects.[7] The distortion is significant when the O K_α fluorescent emission is strongly dependent on the incoming photon energies at the TM $L_{2,3}$ regions. To reduce the distortion in spectral line shapes, partial-fluorescence-yield (PFY) and inverse partial-fluorescence-yield (IPFY) modes have been utilized in previous works,[6–14] although the mechanisms of PFY and IPFY are still under debate.[6,8,9,15–19] The PFY detection mode using a silicon-drift detector (SDD) can select a specific emission, e.g. TM $L_{\alpha,\beta}$, suppressing the influence of the O K_α emission. The distortions in the line shape of L_3-edge XAS can be further reduced by use of IPFY detection that is the inversed intensity of O K_α emission.[6–12]

In this study, we select $LiFePO_4$ and $LiNi_{0.5}Mn_{1.5}O_4$ as model examples to investigate those effects in TFY mode and utilities of PFY and IPFY modes. $LiFePO_4$ is a promising cathode material because of the low-cost constituent element and the highly stable charge-discharge properties.[20] In the olivine-type crystal structure, the Fe atoms are located in the FeO_6 octahedrons and should be divalent. Spinel-type $LiNi_{0.5}Mn_{1.5}O_4$ is an attractive cathode material in terms of the high voltage of ~4.8 V vs. Li/Li^+.[21] The Ni and Mn atoms also form the $(Ni,Mn)O_6$ octahedrons with O_h symmetry. The formal valences of Ni and Mn for the initial state are considered as 2+ and 4+, respectively. In addition, we performed the Cr L-edge XAS for $Li_{0.35}Mn^{4+}{}_{0.65}Cr^{3+}{}_{0.35}O_2$[22] to judge the utility of FY modes at Cr L edges.

We demonstrate TFY, PFY and IPFY XAS for those as-synthesized typical cathode materials in order to discuss appropriate use of the FY modes for each material/element. In this study, we focus on trends in the TMs of the cathode materials as observed in the FY XAS spectra.

$LiFePO_4$ was synthesized with a solid-state reaction method.[23] $LiNi_{0.5}Mn_{1.5}O_4$ was synthesized by an electrospinning method.[24] We confirmed the successful syntheses of the cathode materials using powder X-ray diffraction and electrochemical experiments. The fabrication process of $Li_{0.35}Mn_{0.65}Cr_{0.35}O_2$ has been described elsewhere.[22] We also prepared a charged sample of $LiNi_{0.5}Mn_{1.5}O_4$. The electrochemical experiments were performed by the same procedures described in Ref. 24.

For $LiFePO_4$ and $LiNi_{0.5}Mn_{1.5}O_4$, TEY, PFY, and IPFY XAS measurements were performed at BL-7A of the Photon Factory. The energy resolution of incident photon energies for the XAS measurements was $E/\Delta E \sim 1500$. An SDD was used for the PFY and IPFY detection. The energy width of SDD profile for fixed incident energies is approximately 100 eV. TFY XAS measurements were carried out at BL7.0.1 and BL8.0.1 of the Advanced Light Source with an energy resolution of $E/\Delta E \sim 2000$ for the incident photon energies. A photodiode was used for the detection of TFY system.

For $Li_{0.35}Mn_{0.65}Cr_{0.35}O_2$, TEY, TFY PFY, and IPFY XAS experiments were performed at 11ID-1 Spherical Grating Monochromator (SGM) of the Canadian Light Source. The TFY spectra

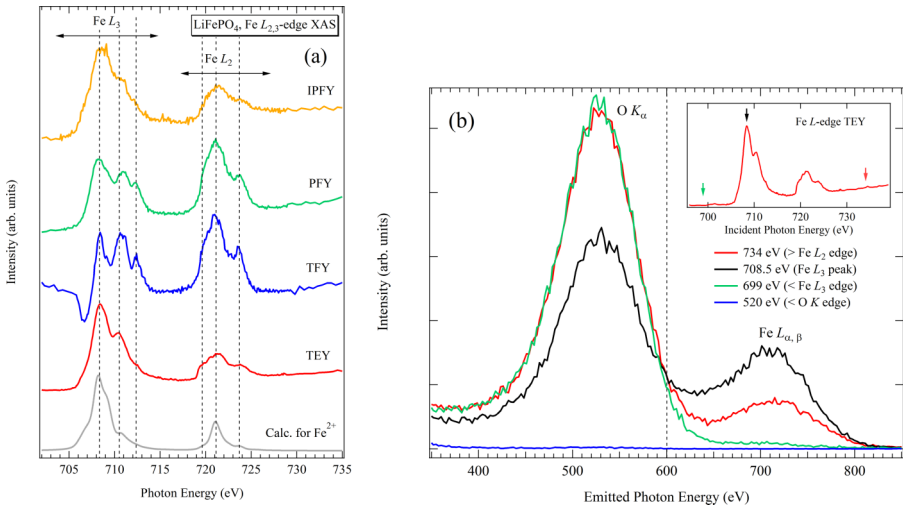

FIG. 1. (a) The Fe $L_{2,3}$-edge XAS spectra for $LiFePO_4$ taken by TEY, TFY, PFY and IPFY detection modes. Calculated spectrum for Fe^{2+} HS state is also shown. (b) Emitted-photon-energy ($h\nu_{out}$) profiles for several incident photon energies ($h\nu_{in}$). The corresponding incident energies are indicated in the inset: TEY spectrum.

were measured with a channel plate detector. The IPFY spectra were measured using an SDD with an energy width of ~120 eV. The energy resolution of incident photon energies was set to 5000. All the XAS measurements were performed at room temperature. Configuration-interaction full-multiplet (CIFM) calculations were adopted for the analysis of the $L_{2,3}$-edge XAS spectra.[25–28] Ligand-to-metal charge transfer (LMCT) was taken into account in the calculation.

Figure 1(a) shows the Fe $L_{2,3}$-edge TEY, TFY, PFY, and IPFY XAS spectra for $LiFePO_4$. The main peak at 708.5 eV in the TEY spectrum is assigned to Fe^{2+} high-spin (HS) state from the multiplet calculation while the peak at 710.5 eV is slightly larger than the calculated Fe^{2+} HS spectrum. Most likely, a small fraction of Fe^{3+} HS should coexist according to previous reports.[29,30] The TFY spectrum exhibits a dip-like structure at 706.5 eV and less pronounced L_3 peaks at 708.4 and 710.5 eV. The L_3 peak intensity is similar to that in the L_2 edge. In the PFY spectrum corresponding to the Fe $L_{\alpha,\beta}$ emission, the dip-like structure at 706.5 eV was not observed although the L_3/L_2 intensity ratio is similar to that in the TFY spectrum and smaller than that in TEY. On the other hand, the IPFY spectrum which is the inverse of the O K_α emission shows the TEY-like intensity ratio of L_3/L_2. Furthermore, the profile of the IPFY spectrum is almost the same as that of TEY, suggesting the bulk and surface electronic structures are identical. These results indicate that the saturation and self-absorption effects are emphasized at the Fe L edge of this material. IPFY can be the most appropriate method to detect the bulk Fe 3d states. The results are consistent with the data collected by Yang *et al.*[7]

Figure 1(b) shows the emitted-photon-energy ($h\nu_{out}$) profiles taken at three incident photon energies ($h\nu_{in}$). Each profile was measured for 1 min. Although the energy width of the SDD profile is about 100 eV, the O K_α and Fe $L_{\alpha,\beta}$ emissions can be distinguished. The O K_α and Fe $L_{\alpha,\beta}$ emissions were not observed for $h\nu_{in}$ = 520 eV because 520 eV is lower than the O K edge absorption threshold. For $h\nu_{in}$ = 699 eV (below the Fe L_3 edge), only the O K_α emission is detected. The Fe $L_{\alpha,\beta}$ emission (for 600 < $h\nu_{out}$ < 800 eV) is enhanced for $h\nu_{in}$ = 708.5 eV corresponding to the Fe L_3 edge, while O K_α emission (for 420 < $h\nu_{out}$ < 600 eV) is considerably reduced. The ~40% reduction of O K_α emission causes the apparent reduction of Fe L_3 peak in the TFY spectrum. In addition, compared with the profile for $h\nu_{in}$ = 708.5 eV, the Fe $L_{\alpha,\beta}$ and O K_α emission intensities were reduced and unchanged for $h\nu_{in}$ = 734 eV, respectively. This is consistent with the Fe L_2 TFY and PFY spectra which show high intensities.

As Fig. 2(a) shows, the Mn $L_{2,3}$-edge TEY spectrum is attributed to a Mn^{4+} state. However, the TFY spectrum exhibits a considerable deformation at the Mn L_3 edge, suggesting that the self-absorption and saturation effects strongly affect the Mn L_3-edge TFY spectrum. The IPFY

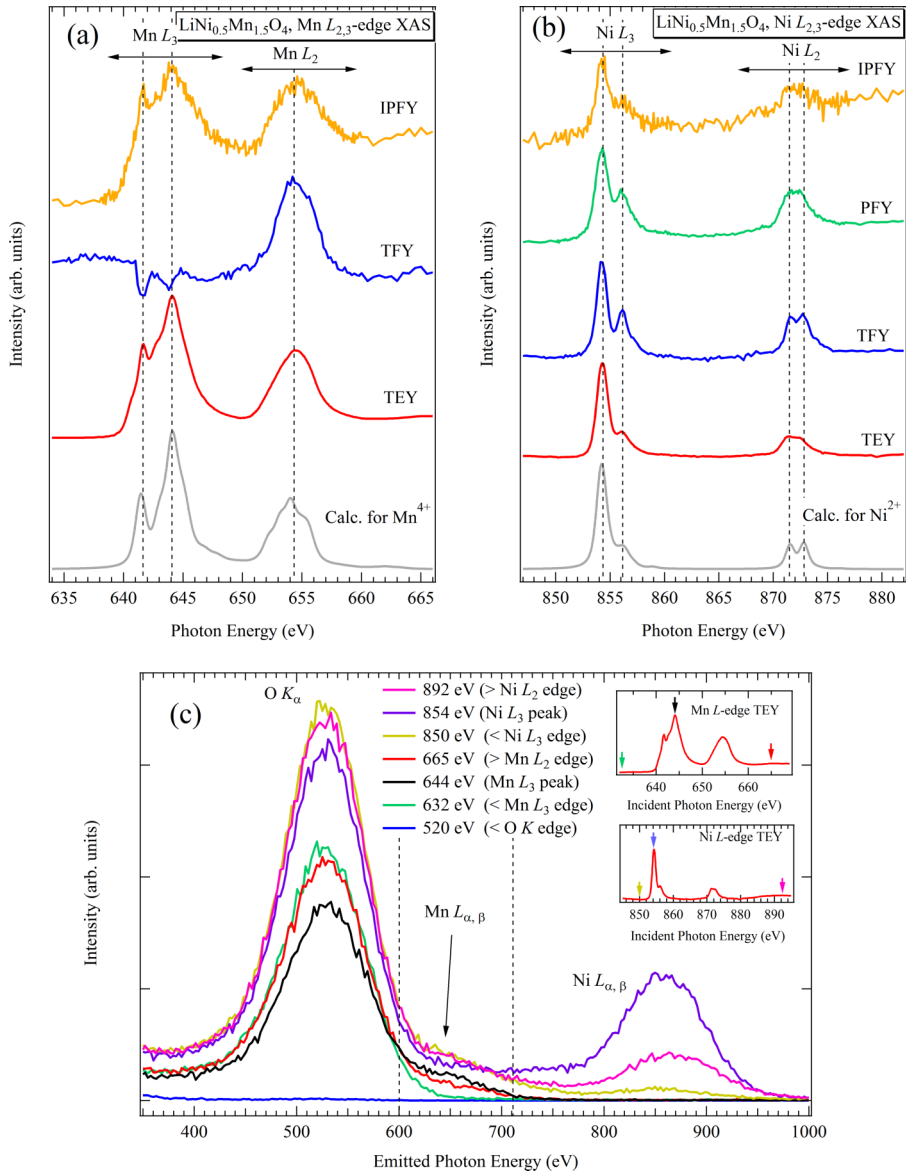

FIG. 2. (a) The Mn $L_{2,3}$-edge and (b) Ni $L_{2,3}$-edge XAS spectra for $LiNi_{0.5}Mn_{1.5}O_4$ taken by TEY, TFY, PFY and IPFY detection modes. Calculated spectra are also shown. (c) Emitted-photon-energy ($h\nu_{out}$) profiles for several incident photon energies ($h\nu_{in}$). The corresponding incident energies are indicated in the insets: TEY spectra.

spectrum displays a clear Mn L_3-edge structure although the L_3/L_2 intensity ratio is slightly smaller than that in TEY. The IPFY spectrum is also assigned to the Mn^{4+} state. The similarity between TEY and IPFY spectra indicates that the surface and bulk electronic structures are almost identical.

The Ni $L_{2,3}$-edge TEY spectrum exhibits the Ni^{2+} HS multiplet structure (Fig. 2(b)). In contrast to the Mn L edge, the distortions of the Ni L_3 edge TFY and PFY spectra are suppressed. Although the L_3/L_2 intensity ratios of TFY and PFY are slightly smaller than that for TEY, the TFY and PFY spectra are available for the analysis using the multiplet calculations. The IPFY spectrum is also similar to the TFY and PFY spectra. However, the signal-to-noise (S/N) ratio of IPFY spectrum is lower than those of TFY and PFY spectra. Thus, the IPFY detection mode is less advantageous for the analysis of Ni $L_{2,3}$ edges of this material.

Figure 2(c) shows the $h\nu_{out}$ profiles of emissions taken at several $h\nu_{in}$. The O K_α, Mn $L_{\alpha,\beta}$ and Ni $L_{\alpha,\beta}$ emissions can be observed. The Mn $L_{\alpha,\beta}$ emissions (for $600 < h\nu_{out} < 720$ eV) are

enhanced at $h\nu_{in}$ = 644 eV. However, the degree of enhancement is lower than the degree of reduction of the O K_α emission, leading to the deformation at the Mn L_3 edge in the TFY spectrum. On the other hand, at the Ni L_3 edge, the degree of reduction of the O K_α emission becomes small and the Ni $L_{\alpha,\beta}$ emission (for 750 < $h\nu_{out}$ < 970 eV) increases considerably, such that the deformations at the Ni L_3 edge in the TFY and PFY spectra are less pronounced.

The Mn L_3-edge TFY XAS spectrum for $LiNi_{0.5}Mn_{1.5}O_4$ exhibits the large distortions in XAS line shapes, suggesting that the XAS line shapes of Mn L_3 edge in Li-TM oxides (and phosphates) should be very sensitive to the self-absorption and saturation effects, while these effects depend on the density and composition of sample and experimental geometries. This is consistent with the Mn L_3 edge/$L_{\alpha,\beta}$ emission (~640 to ~660 eV) being very near O K edge/K_α emission (~525 to ~560 eV) in photon energy. The Fe L_3 edge XAS is also sensitive, although the influence of self-absorption and saturation effects should be smaller than that in the MnL_3 edge. Considering the present results, the IPFY detection mode can become powerful tools for the Mn and Fe $L_{2,3}$-edge measurements. In the case of Ni $L_{2,3}$ edges, the TFY and PFY detection modes should be more appropriate than IPFY mode in terms of the S/N ratio. Most likely, Co $L_{2,3}$ edges for Li-TM oxides (and phosphates) including Co would be positioned as the intermediate character between Fe and Ni $L_{2,3}$ edges.

As Fig. 2(c) indicates, the $h\nu_{in}$ dependence of O K_α emission weakens as $h\nu_{in}$ increases. To further verify this tendency, we also performed the Cr L-edge XAS for $Li_{0.35}Mn_{0.65}Cr_{0.35}O_2$ (Fig. 3(a)). The TEY spectrum is attributed to the Cr^{3+} state. On the other hand, not only the L_3 edge, but also the L_2 edge is reversed with negative sign in the TFY spectrum, which is more problematic than the case of Mn L-edges (Fig. 3(b)). The Cr L edges (~575 to ~595 eV) are so close to the O K edge (~525 to ~560 eV) that the Cr $L_{\alpha,\beta}$ emission cannot be separated from the O K_α emission within the energy width of SDD (~100 eV) (Fig. 3(c)). The Cr L-edge IPFY spectrum in Fig. 3(a) is composed by extracting the structure below 570 eV in Fig. 3(c) as the OK_α emission. However, the S/N ratio and L_3/L_2 intensity ratio are not ideal. If the energy resolution of the detector is improved, for example by using a high-resolution soft X-ray emission spectrometer,[31,32] then the separation of Cr $L_{\alpha,\beta}$ emissions from O K_α emission should be facilitated.

Figure 4 summarizes the utilities of TFY, PFY and IPFY for each TM L edge of Li-TM oxides/phosphates. Note that the tendency is limited to powdered Li-TM oxides/phosphates with particle sizes between 10 nm and 10 μm generally used as cathode materials of LIB. The IPFY mode can be useful for Cr, Mn, and Fe L edges for those materials. For L edges with higher energies, TFY and PFY are more suitable than IPFY. In addition, TFY and PFY should be available for Ti and V without any problems because these early TMs' L edges are located below the O K edge. Appropriate choice of the FY modes is inevitable to study the bulk electronic structures of Li-TM oxides and related materials. As Fig. 5 shows, the bulk electronic structure is often different from the surface electronic structure in particular for charged (or discharged) samples. In the case of $LiNi_{0.5}Mn_{1.5}O_4$ (Fig. 5), the degree of oxidation of Ni due to the charge reaction is different between the surface and bulk. The Ni L-edge TFY XAS spectrum for the charged state shows enhanced peaks at 856 and 873 eV, indicating partial oxidation reaction of $Ni^{2+} \rightarrow Ni^{3+}$[33] in the bulk region. On the other hand, in the surface-sensitive TEY mode, the line shape attributed to the Ni^{2+} state is almost maintained for the charged state, suggesting existence of redox-inactive Ni and/or some side reactions such as NiO formation near the surface. Thus, a combined use of TEY and FY is essential for the electronic-structure analyses of the electrode materials.

In conclusion, we demonstrated TEY, TFY, PFY and IPFY XAS studies for powdered several Li-TM oxides and a phosphate which are cathode materials for LIBs. The utilities of FY modes strongly depend on the element (edge) and material (composition). The FY modes should be carefully chosen for each material. The distortion of Ni L_3-edge TFY XAS line shapes is not large whereas Cr, Mn and Fe L_3-edge TFY XAS are greatly affected. We conclude that, in the FY XAS studies of the cathode materials, the IPFY XAS is most appropriate for the Cr, Mn, and Fe L edges and the TFY and PFY XAS modes are available enough for the Ni L edge which is far from the O K edge. This consideration will contribute to TM L-edge FY XAS studies of charged/discharged samples for novel electrode materials.

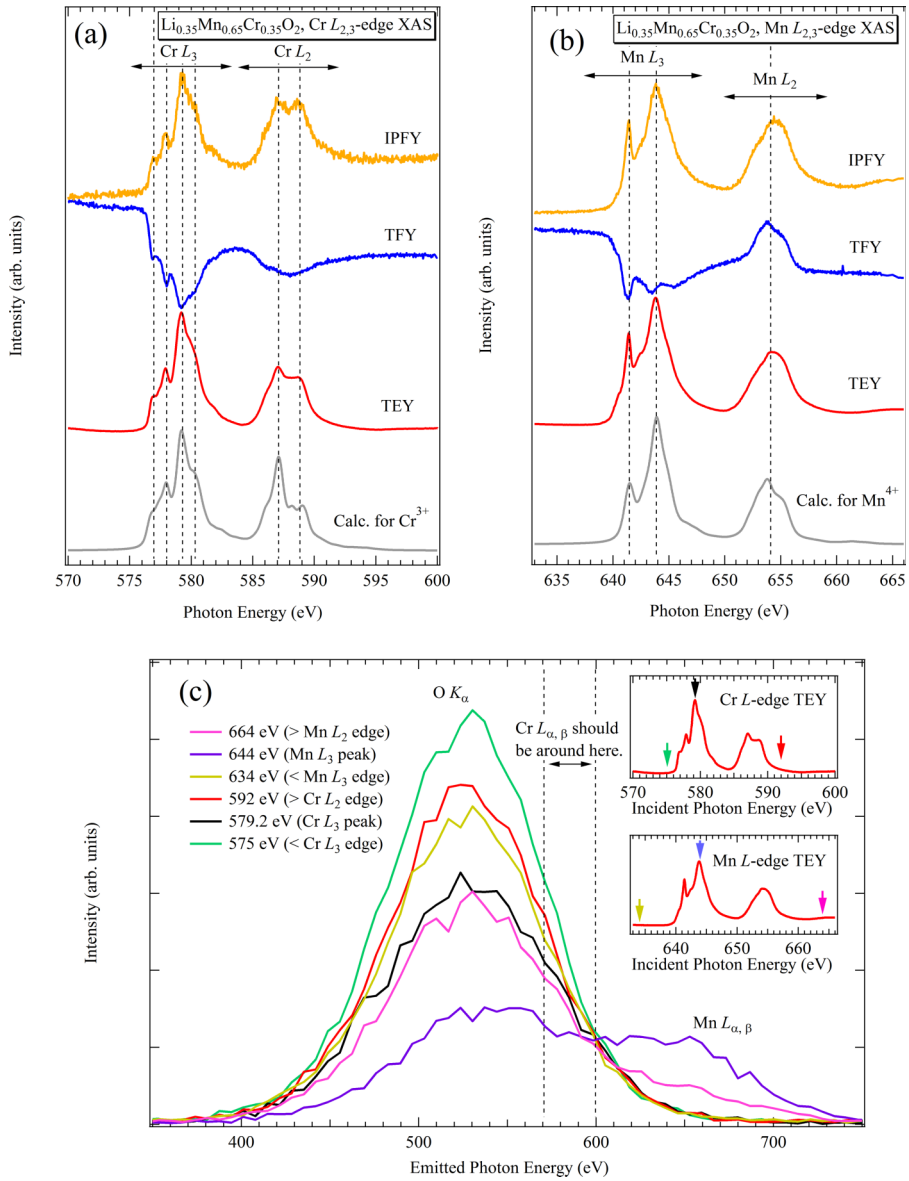

FIG. 3. (a) The Cr $L_{2,3}$-edge and (b) Mn $L_{2,3}$-edge XAS spectra for $Li_{0.35}Mn_{0.65}Cr_{0.35}O_2$. (c) Emitted-photon-energy ($h\nu_{out}$) profiles for several incident photon energies ($h\nu_{in}$). The Cr $L_{\alpha,\beta}$ emission should be around 580 eV, which cannot be separated from the O K_α emission in the present energy resolution.

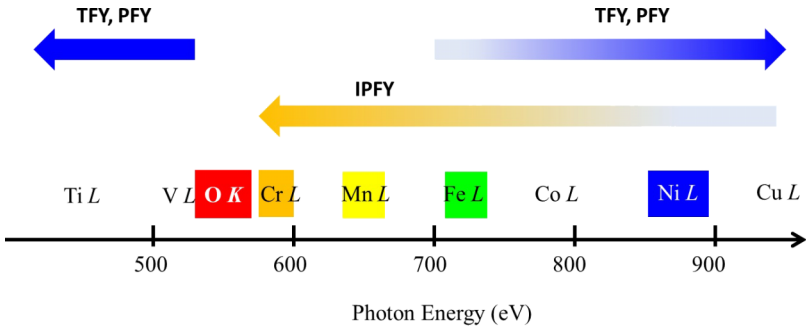

FIG. 4. A scheme of utilities of TFY, PFY and IPFY for each TM L edge of powdered Li-TM oxides/phosphates (Ti, V, Co and Cu L edges are not investigated here). The color scales of the arrows indicate the utilities of each XAS mode.

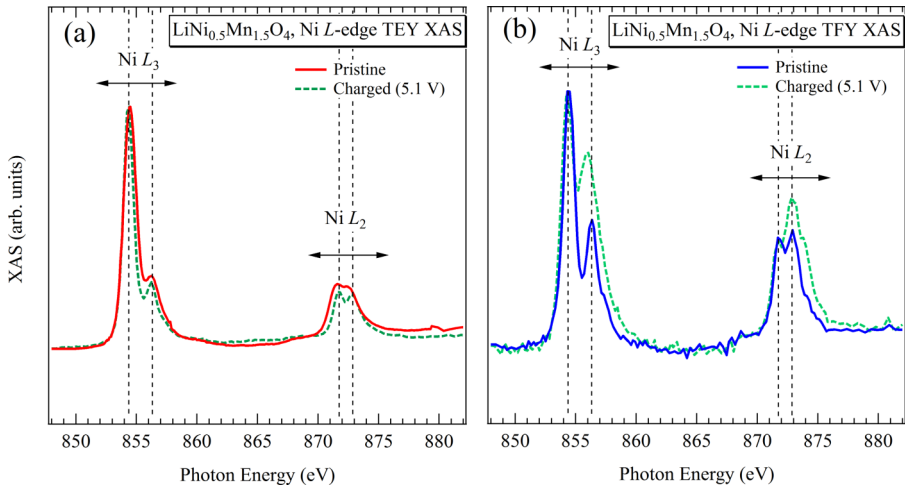

FIG. 5. The Ni *L*-edge XAS spectra for the pristine and charged $LiNi_{0.5}Mn_{1.5}O_4$ recorded by (a) the TEY and (b) TFY modes. The spectra were normalized at 854.2 eV to emphasize the differences at 856 and 873 eV in (b).

ACKNOWLEDGEMENTS

This work was performed under the approvals of the Photon Factory Program Advisory Committee (Proposal Nos. 2012G107, 2013G169 and 2014G100) and the Advanced Light Source (Proposal No. 04907R). The Advanced Light Source is supported by the Director, Office of Science, Office of Basic Energy Sciences, of the U.S. Department of Energy under Contract No. DE-AC02-05CH11231. Research described in this paper was partly performed at the Canadian Light Source, which is supported by CFI, NSERC, the University of Saskatchewan, the Government of Saskatchewan, WD, NRC, and CIHR. The synthesis work at NREL was supported by the NREL LDRD Program. This work was also conducted based on the Japan-U.S. cooperation project for research and standardization of Clean Energy Technologies.

[1] Y. Shiraishi, I. Nakai, T. Tsubata, T. Himeda, and F. Nishikawa, J. Solid State Chem. **133**, 587 (1997).
[2] A. Ito, Y. Sato, T. Sanada, M. Hatano, H. Horie, and Y. Osawa, J. Power Sources **196**, 6828 (2011).
[3] F. de Groot and A. Kotani, *Core Level Spectroscopy of Solids (Advances in Condensed Matter Science)* (CRC Press Taylor & Francis Group, Boca Raton, FL, 2008).
[4] F. M. F. de Groot, J. Electron Spectrosc. Relat. Phenom. **67**, 529 (1994).
[5] S. Eisebitt, T. Boske, J.-E. Rubensson, and W. Eberhardt, Phys. Rev. B **47**, 14103 (1993).
[6] H. Wadati, A. J. Achkar, D. G. Hawthorn, T. Z. Regier, M. P. Singh, K. D. Truong, P. Fournier, G. Chen, T. Mizokawa, and G. A. Sawatzky, Appl. Phys. Lett. **100**, 193906 (2012).
[7] S. Yang, D. Wang, G. Liang, Y. M. Yiu, J. Wang, L. Liu, X. Sun, and T.-K. Sham, Energy Environ. Sic. **5**, 7007 (2012).
[8] A. J. Achkar, T. Z. Regier, H. Wadati, Y.-J. Kim, H. Zhang, and D. G. Hawthorn, Phys. Rev. B **83**, 081106 (2011).
[9] A. J. Achkar, T. Z. Regier, E. J. Monkman, K. M. Shen, and D. G. Hawthorn, Sci. Rep. **1**, 182 (2011).
[10] S. I. Bokarev, M. Dantz, E. Suljoti, O. Kühn, and E. F. Aziz, Phys. Rev. Lett. **111**, 083002 (2013).
[11] P. Wernet, K. Kunnus, S. Schreck, W. Quevedo, R. Kurian, S. Techert, F. M. F. de Groot, M. Odelius, and A. Fohlisch, J. Phys. Chem. Lett. **3**, 3448 (2012).
[12] D. Perk and T. Regier, Environ. Sci. Technol. **46**, 3163 (2012).
[13] C. Yogi, D. Takamatsu, K. Yamanaka, H. Arai, Y. Uchimoto, K. Kojima, I. Watanabe, T. Ohta, and Z. Ogumi, J. Power Sources **248**, 994 (2014).
[14] H. Wadati, D. G. Hawthorn, T. Z. Regier, G. Chen, T. Hitosugi, T. Mizokawa, A. Tanaka, and G. A. Sawatzky, Appl. Phys. Lett. **97**, 022106 (2010).
[15] E. F. Aziz, M. H. Rittmann-Frank, K. M. Lange, S. Bonhommeau, and M. Chergui, Nature Chem. **2**, 853 (2010).
[16] T. Z. Regier, A. J. Achkar, D. Peak, J. S. Tse, and D. G. Hawthorn, Nature Chem. **4**, 765 (2012).
[17] F. M. F. de Groot, Nature Chem. **4**, 766 (2012).
[18] E. F. Aziz, K. M. Lange, S. Bonhommeau, and M. Chergui, Nature Chem. **4**, 767 (2012).
[19] R. Kurian, K. Kunnus, P. Wernet, S. M. Butorin, P. Glatzel, and F. M. F. de Groot, J. Phys. Condens. Matter **24**, 452201 (2012).
[20] A. Padhi, K. Nanjundaswamy, and J. B. Goodenough, J. Electrochem. Soc. **144**, 1188 (1997).
[21] Q. M. Zhong, A. Bonakdarpour, M. J. Zhang, Y. Gao, and J. R. Dahn, J. Electrochem. Soc. **144**, 205 (1997).
[22] F. Du, Z.-F. Huang, C.-Z. Wang, X. Meng, and G. Chen, J. Appl. Phys. **102**, 113906 (2007).
[23] C. Ban, W.-J. Yin, H. Tang, S.-H. Wei, Y. Yan, and A. C. Dillon, Adv. Energy Mater. **2**, 1028 (2012).

[24] E. Hosono, T. Saito, J. Hoshino, Y. Mizuno, M. Okubo, D. Asakura, K. Kagesawa, D. Nishio-Hamane, T. Kudo, and H. S. Zhou, CrystEngComm **15**, 2592 (2013).
[25] Y. Nanba and K. Okada, J. Phys. Soc. Jpn. **79**, 114722 (2010).
[26] Y. Nanba and K. Okada, J. Electron Spectrosc. Relat. Phenom. **185**, 167 (2012).
[27] Y. Nanba, D. Asakura, M. Okubo, Y. Mizuno, T. Kudo, H. S. Zhou, K. Amemiya, J.-H. Guo, and K. Okada, J. Phys. Chem. C **116**, 24896 (2012).
[28] Y. Nanba, D. Asakura, M. Okubo, H. S. Zhou, K. Amemiya, K. Okada, P.-A. Glans, C. A. Jenkins, E. Arenholz, and J.-H. Guo, Phys. Chem. Chem. Phys. **16**, 7031 (2014).
[29] X. Liu, J. Liu, R. Qiao, Y. Yu, H. Li, L. Suo, Y.-s. Hu, Y.-D. Chuang, G. Shu, F. Chou, T.-C. Weng, D. Nordlund, D. Sokaras, Y. J. Wang, H. Lin, B. Barbiellini, A. Bansil, X. Song, Z. Liu, S. Yan, G. Liu, S. Qiao, T. J. Richardson, D. Prendergast, Z. Hussain, F. M. F. de Groot, and W. Yang, J. Am. Chem. Soc. **134**, 13708 (2012).
[30] S. Kurosumi, N. Nagamura, S. Toyoda, K. Horiba, H. Kumigashira, M. Oshima, S. Furutsuki, S.-i. Nishimura, A. Yamada, and N. Mizuno, J. Phys. Chem. C **115**, 25519 (2011).
[31] G. Ghiringhelli, A. Piazzalunga, C. Dallera, G. Trezzi, L. Braicovich, T. Schmitt, V. N. Strocov, R. Betemps, L. Patthey, X. Wang, and M. Grioni, Rev. Sci. Instrum. **77**, 113108 (2006).
[32] Y. Harada, M. Kobayashi, H. Niwa, Y. Senba, H. Ohashi, T. Tokushima, Y. Horikawa, S. Shin, and M. Oshima, Rev. Sci. Instrum. **83**, 013116 (2012).
[33] C. Piamonteze, F. M. F. de Groot, H. C. N. Tolentino, A. Y. Ramos, N. E. Massa, J. A. Alonso, and M. J. Martínez-Lope, Phys. Rev. B **71**, 020406(R) (2005).